Experimental Investigation of Small Diameter Two-Phase Closed Thermosyphons Charged with Water, FC-84, FC-77 & FC-3283

Hussam Jouhara

School of Engineering and Design, Brunel University, Uxbridge, Middlesex, UB8 3PH, UK,
Tel: +44 1895 267656, Fax: +44 1895 256392, Email: hussam.jouhara@brunel.ac.uk

Anthony J. Robinson

Department of Mechanical and Manufacturing Engineering, Trinity College Dublin, Ireland,
Tel: +353 1 896 3919, Fax: +353 1 679 5554, Email: arobins@tcd.ie

Submitted to:

Abstract

An experimental investigation of the performance of thermosyphons charged with water as well as the dielectric heat transfer liquids FC-84, FC-77 and FC-3283 has been carried out. The copper thermosyphon was 200 mm long with an inner diameter of 6 mm, which can be considered quite small compared with the vast majority of thermosyphons reported in the open literature. The evaporator length was 40 mm and the condenser length was 60 mm which corresponds with what might be expected in compact heat exchangers. With water as the working fluid two fluid loadings were investigated, that being 0.6 ml and 1.8 ml, corresponding to approximately half filled and overfilled evaporator section in order to ensure combined pool boiling and thin film evaporation/boiling and pool boiling only conditions respectively. For the Flourinert^{TM} liquids, only the higher fill volume was tested as the aim was to investigate pool boiling opposed to thin film evaporation. Generally, the water charged thermosyphon evaporator and condenser heat transfer characteristics compared well with available predictive correlations and theories. The thermal performance of the water charged thermosyphon also outperformed the other three working fluids in both the effective thermal resistance as well as maximum heat transport capabilities. Even so, FC-84, the lowest saturation temperature fluid tested, shows marginal improvement in the heat transfer at low operating temperatures. All of the tested Flourinert^{TM} liquids offer the advantage of being dielectric fluids, which may be better suited for sensitive electronics cooling applications and were all found to provide adequate thermal performance up to approximately 30-50 W after which liquid entrainment compromised their performance.

Nomenclature

Symbol

A	Surface area (m²)			

A Surface area (m²)

C_p Specific heat (J/kgK)

D Diameter (m)

d_d Bubble departure (m)

g Gravitational acceleration (m/s²)

h Heat transfer coefficient (W/m²K)

h_{fg} Latent heat of vaporisation (J/kg)

I Current (A)

k Thermal conductivity (W/mK)

l Length (m)

L_b bubble length scale (m)

$\dot{m}$ Mass flow rate (kg/s)

P Pressure (Pa)

Q Heat transfer rate (W)

q Heat flux (W/m²)

R Thermal resistance (K/W)

T Temperature (°C)

V Voltage (V)

Greek Symbols

β Contact angle (°)

μ Dynamic viscosity (N s/m²)

ρ Density (kg/m³)

σ Surface tension (N/m)

Subscripts

atm Atmospheric

av Average value

c Condenser section

cs Cross section

e Evaporator section

exp Experimental

f Film

l Liquid

$Pred$ Predicted

v Vapour

sat Saturation

w Water

1. Introduction

Thermosyphons are enclosed, passive two phase heat transfer devices. They make use of the highly efficient thermal transport process of evaporation and condensation to maximize the thermal conductance between a heat source and a heat sink. They are often referred to as thermal superconductors or thermal 'short-circuits' because they can transfer large amounts of heat over relatively large distances with small temperature differences between the heat input and heat output zones. The amount of heat that can be transported by these devices is normally several orders of magnitude greater than pure conduction through a solid metal [1;2]. They are proven to be very effective, low cost and reliable heat transfer devices for applications in many thermal management and heat recovery systems. Their usage is essential in the cooling of high-performance electronics components, heat exchangers in waste heat recovery applications and solar energy systems, to name a few [2].

A cross section of a closed two-phase thermosyphon is illustrated in Fig. 1. The thermosyphon consists of an evacuated sealed tube that contains a small amount of liquid. The heat applied at the evaporator section is conducted across the pipe wall causing the liquid in the thermosyphon to boil in the liquid pool region and evaporate and/or boil in the film region [3]. In this way the working fluid absorbs the applied heat load converting it to latent heat. The vapour in the evaporator zone is at a higher pressure than in the condenser section causing the vapour to flow upward. In the cooler condenser region the vapour condenses thus releasing the latent heat that was absorbed in the evaporator section. The heat then conducts across the thin liquid film and exits the thermosyphon through the tube wall and into the external environment. Within the tube, the flow circuit is completed by the liquid being forced by gravity back to the evaporator section in the form of a thin liquid film. As the thermosyphon relies on gravity to pump the liquid back to the evaporator section, it cannot operate at inclinations close to the horizontal position.

The heat transfer within the thermosyphon depends on the complex phase change process in the evaporator and condenser regions, which can be complicated by the counter flow of the liquid and vapour phases. As outlined by El-Genk and Saber [3], the evaporator section is possibly the most complex and least well understood portion of the thermosyphon as it must incorporate the separate effects of pool boiling in the lower region as well as laminar convection and/or boiling within the continuous

liquid film. To predict the heat transfer coefficients within the evaporator section empirical or semi-empirical correlations are generally applied. Liquid pool boiling correlations, such as those of Rohsenow [4], Kutateladze [5] and Shiraishi et al [6], among many others, have been used with varying degrees of success. In the liquid film, the heat transfer can be significantly higher than in the pool region and depends on the mode of heat transfer which can range from natural convection at low heat fluxes to nucleate boiling at high heat fluxes [3]. For the low enough heat fluxes, an extension of Nusselt's falling film theory or simple modifications of it are suggested [3;6]. For high heat fluxes where nucleate boiling occurs in the film, El-Genk and Saber [3] have provided a useful correlation which have shown to predict heat transfer coefficients that are an order of magnitude higher that the predictions of the pool boiling correlation of Kutateladze [5]. For boiling in small diameter tubes where confinement will influence the boiling heat transfer, Chowdhury et al [6] have developed correlations for water, ethanol and R113.

The heat transfer coefficient in the condenser region is generally predicted using Nusselt's theory for filmwise condensation provided the film Reynolds number is sufficiently low [7;8]. For higher Reynolds numbers waviness and turbulence may enhance the heat transfer and correlations exist to predict these [8]. Even still, much of the empirical data is over predicted by Nusselt's theory at low Reynolds numbers [8;9] which may partially be explained by the work of Hashimoto and Kaminaga [9] who proved that liquid entrainment can deteriorate the condensation heat transfer for low Reynolds numbers.

Most of the published literature on the thermal-hydraulic behaviour of thermosyphons involves the use of rather large diameter units. This is likely because the target technologies, such as heat recovery systems, were large in scale demanding large heat exchangers. However, applications such as electronics thermal management and automotive heat recovery require much more compact heat exchangers demanding the implementation of smaller diameter and shorter thermosyphons. Further to this, some sensitive applications may require the use of working fluids other than water. In some instances, in particular low operating temperatures, it has even been shown that water gives less satisfactory heat transfer performance compared with low saturation temperature fluids [10].

Some publications exist concerning experimental work on the performance of thermosyphons with different working fluids. The most common thermosyphon

working fluids is water due to its high figure of merit, availability, cost and non-toxic and environmentally neutral properties. Even still, earlier work also studied possible working fluids for low to intermediate operating temperatures including, but not limited to, R-11, R-12, R-22, R113 [6;7;10-15], as well as ethanol [6;7]. Because of their negative environmental impact and/or toxicity, the early Freon range has on the most part been prohibited and replaced by more environmentally friendly and low to non-toxic fluids such as R134a and 3M Fluorinert[TM] liquids. R134a has been tested as a thermosyphon working fluid by some researchers including Abou-Ziyan et al. [16] and Ong and Haider-E-Alahi [17]. The use of environmentally sound and non-toxic 3M Fluorinert[TM] heat transfer liquids has not been extensively reported in the open literature. The thermal performance of relatively large thermosyphons charged with FC-72 was reported by Park et al. [18;19] for the thermal management of high power semiconductors. However, for the range of Fluorinert[TM] heat transfer liquids with varying boiling points there appears to be a lack of information in the open literature. In particular, there is no information regarding their use in compact, small diameter thermosyphons.

In this paper, the thermal performance of copper thermosyphons charged with water as well as three Fluorinert[TM] liquids, FC-77, FC-84 and FC-3283, is reported for a small thermosyphon (length=200 mm, inner diameter=6mm). The physical size of the instrumented thermosyphons is typical for compact heat exchanger devices such as those required for thermal management of electronics, for example. Fluorinert liquids were chosen for testing since they are dielectric and cover a range of thermophysical properties, in particular a boiling points in a range of 80ºC to 128ºC. Water tests are performed with two fluid loadings; with evaporator section overfilled to ensure pool boiling and; with the evaporator, approximately half filled to have a liquid pool and liquid film region. For the cases of the Fluorinert[TM] working fluids, all tests were performed with the evaporator overfilled to ensure pool-boiling conditions. Various correlations for predicting the heat transfer in the evaporator and condenser sections are compared with the experimental measurements and the thermal performance characteristics of all four working fluids are compared.

2. Experimental Apparatus

Fig. 2 shows a schematic diagram of the experimental apparatus used in this investigation. The apparatus consists of the thermosyphon, heater, cooling water flow

circuit and instrumentation. The 6 mm inside diameter thermosyphon was manufactured by drilling a 200mm long hole in the centre of a solid copper rod with an outside diameter of 12mm. This facilitated sealing the bottom end of the device while at the same time allowing the top end to be machined with a $^1/_{16}{}''$ NPT thread, which facilitated the Schrader valve for charging the thermosyphon with different fluids and different fluid loadings.

The fluids tested were water, FC-84, FC-77 and FC-3283. Water was chosen as a reference fluid with which other fluids can be compared. The Flourinert liquids were selected based on the range of thermophysical properties that they possess. Some of the more crucial properties are listed in Table 1. Of particular interest here is the range of boiling points which ranges from 80 ºC for FC-84 to128 ºC for FC-3283 with FC-77 having a similar boiling point to water.

The fluid loading was kept constant at 1.8 ml for all tests except one set of tests with water in which the loading was 0.6 ml. In non-operational mode 1.8 ml is sufficient volume to overfill the evaporator section. In operational mode, this volume provides enough liquid to wet the evaporator section while at the same time providing adequate liquid for the thin liquid film along the condenser and adiabatic sections.

The condenser section of the thermosyphon was cooled by a flow of water through a 70 mm long plastic water jacket that was designed in a 3D CAD package and printed using an InVision^{TM} 3-D rapid-prototyper. To enhance the water-side convective heat transfer coefficient the water jacket was designed with hundreds of rectangular studs on the inside wall to create mixing of the water flow. Sealing was ensured using high temperature silicon sealant. Condenser water was supplied via a constant-head water tank device. This consisted of a tank, pump and control valves as illustrated in Fig. 2. A water feedback loop was installed to keep the water head constant. The flow rate of the cooling water was measured using an Omega FTB602 (± 3% rdg) turbine flow meter and was kept constant at 0.08L/min. The temperature of the cold-water inlet was kept constant by a separate copper coil heat exchanger positioned within the water tank with chilled water running through it.

Heat was applied to the thermosyphon at the evaporator end using a 300W electrical band heater. The heater was wrapped around an annular brass block enclosing the evaporator section of the thermosyphon. Thermal paste was used to ensure adequate thermal contact between the heater block and the thermosyphon. The heated and the adiabatic sections were wrapped with several layers of high-

temperature ceramic insulation to minimise heat losses to the ambient. The electrical power input to the heater was controlled using a variable voltage transformer (variac). The power supplied to the evaporator section was monitored by measuring the applied voltage and current to the band heater with two Metrix MX22 multimeters (0–400VAC ± 1% rdg, 0–10 A ± 2.5% rdg).

The temperature distribution along the thermosyphon was measured using six T-type thermocouples. Two thermocouples were also used to monitor the input and the output water temperatures from the water jacket. All of the thermocouple readings were monitored by Fluke 54II digital thermometers (±0.3 ºC).

3. Data Reduction and Experimental Uncertainty

The effective overall thermal resistance of the thermosyphon was calculated by applying the electrical analogue in the form,

$$R_{\text{exp}} = \frac{\bar{T}_e - \bar{T}_c}{Q} \tag{1}$$

Likewise, in the evaporator and condenser regions, the respective thermal resistances were determined with the following expressions,

$$R_e = \frac{\bar{T}_e - \bar{T}_v}{Q} \tag{2}$$

$$R_c = \frac{\bar{T}_v - \bar{T}_c}{Q} \tag{3}$$

Here $\bar{T}_e$ and $\bar{T}_c$ are the average wall temperatures in the evaporator and condenser respectively and T_v is the saturated vapour temperature taken here as the adiabatic wall temperature. In a similar fashion, the average evaporator and condenser heat transfer coefficients are calculated using the expressions;

$$h_e = \frac{Q}{\pi D l_e (\bar{T}_e - \bar{T}_v)} \tag{4}$$

$$h_c = \frac{Q}{\pi D l_c (\bar{T}_v - \bar{T}_c)} \tag{5}$$

An accurate experimental determination of the thermal performance of the thermosyphon requires accurate measurements of the evaporator and condenser temperatures as well as the power transferred along it. Characterizing the evaporator and condenser temperatures is a relatively straightforward task and is obtained by

simply averaging the temperature measurements along the respective sections. As depicted in Fig. 3 for the water thermosyphon, the temperature distribution along the evaporator and condenser sections was relatively uniform so averaging the measurements is justified. Accurately characterizing the thermal power transfer, Q, is a somewhat more complicated task because it is difficult to accurately quantify the energy losses to the ambient surroundings. To provide confidence in the measured value of Q an energy balance was performed which was compared the electrical power supplied to the evaporator with the energy extracted by the cooling water at the condenser section. The input power was calculated using the supply voltage and current measurements from the multimeters such that,

$$Q_{in} = V \cdot I \tag{6}$$

The experimental uncertainty associated with this measurement was determined to be ±3%. The energy removed at the condenser section was determined by performing an energy balance across the condenser section such that,

$$Q_{out} = \dot{m} C_p (T_{w,out} - T_{w,in}) \tag{7}$$

The experimental uncertainty associated with this measurement was primarily governed by the uncertainty in the temperature measurements and ranged between 15% for low power settings and improved to less than 5% for the higher power settings. The results of the energy balance were found to be within ±10% which is generally within the experimental uncertainty of the experiment. It thus seemed to be a conservative estimate to assume that the experimental uncertainty on the measured power was ±10% over the entire range of powers tested. The resulting uncertainty associated with the experimentally determined thermal resistances is summarized in Table 3 for increasing power levels.

5. Water-Charged Thermosyphon

5.1. Temperature Distribution

The performance of the thermosyphon with 1.8 ml of water was initially examined in detail to develop an understanding of how the unit operates in pool boiling mode. The wall temperature distribution along the thermosyphon is shown in Fig. 3. As illustrated, the wall temperature of the evaporator and condenser sections were approximately uniform for each respective power level tested. The temperature

uniformity is expected considering the uniform temperature phase change process that was occurring within the respective section.

5.2. Heat Transfer

5.2.1. Evaporator Section

There is no correlation or set of correlations that is general enough to predict the nucleate pool boiling heat transfer coefficient in all thermosyphons [14]. It is general practice to choose one or more boiling correlation to compare with the experimental data. The most suitable correlation is then thought to best represent the specific thermal and hydrodynamic conditions for the experimental conditions investigated [1;14;19]. Some correlations, such as those by Imura et al [20], Shiraishi et al [7] and Chowdhury at al [6] were developed specifically for pool boiling in thermosyphons. Interestingly, the correlations developed by Chowdhury et al [6] included confinement effects as the characteristic departure diameters of a bubbles were comparable with the diameter of the tube. Other correlations, such as the well known Rohsenow [4] correlation, included an adjustable constant that depended upon the nature of the surface–fluid combination. Others such as the Kutateladze [5], Labuntsov [21] and Kruzhilin [22] were developed with constants and powers for a wide variety of liquids and boiling conditions which make them more general at the expense of accuracy [23]. Possibly the most general set of pool boiling correlations was developed by Stephan and Abdulsalam [24] where regression analysis was applied to 5000 experimental data points to generate fluid specific heat transfer correlations. Here, the heater type ranged from flat plates, cylinders and wires, all of varying sizes and orientations. For tube diameters much larger than the bubble departure diameter the use of these types of correlations seems rational and often shows relatively good agreement with measurements [1;19;25].

The preponderance of the work in the literature has focused on what can be considered large diameter thermosyphons since the relevant technologies, such as those found in heat recovery and HVAC systems for example, demanded large heat exchangers and thus generally large tube diameters. However, much less is known about scaled-down systems such as those required for electronic cooling applications and compact heat exchangers. Thus, an attempt is made in this work to evaluate the boiling heat transfer in what can be considered a small diameter thermosyphon. The condition for the thermosyphon to be considered 'small' can loosely be defined as the

condition whereby the expected bubble departure diameter is about the same size (or larger) as the radius of the tube,

$$\frac{d_d}{(D/2)} \sim 1 \qquad (8)$$

The rationale behind this is that for the case where $d_d/(D/2) \ll 1$ one would expect that bubbles located diametrically opposed to one another would not influence each other's behaviour. However, for $d_d/(D/2) \sim 1$ or more, one would expect that bubbles facing one another would influence each other's behaviour and subsequent heat transfer.

The departure diameter in Eq. 8 can be roughly estimated from the conventional expression [6],

$$d_d = 0.0204 L_b \beta \qquad (9)$$

where $L_b = [\sigma/g(\rho_l - \rho_g)]^{1/2}$ is the bubble length scale and the contact angle for water has been chosen as $\beta = 45^o$ [6;24]. For the range of water conditions tested, the departure diameter ranged between $0.22mm \leq d_d \leq 0.25mm$ such that $0.73 \leq d_d/(D/2) \leq 0.83mm$ so the thermosyphon in this work can be considered small.

The aim of this work is not to perform an exhaustive comparison of all nucleate pool boiling correlations. Instead, a cross section of the correlations available in the open literature, in particular those which appear frequently in thermosyphon publications, have been included to obtain a sense of their applicability for the situation under study. For ease of reference, the selected correlations are listed in Table 3. Fig. 4 shows the comparison between the predicted and measured thermal resistance values where the filled markers represent correlations developed specifically for nucleate boiling in thermosyphons. The thermal resistance is determined by calculating the heat transfer coefficient and then using the following expression;

$$R_e = \frac{1}{h_e(\pi D l_e)} \qquad (10)$$

Generally the experiments and predictions show reasonable agreement with the majority of the points being within the ±30% band. For the thermosyphon-based correlations, the Imura et al [20] and Shiraishi et al [7] correlations are comparable and under-predict the measurements when the resistance is low i.e. for the highest heat flux cases. Agreement worsens as the thermal resistance gets larger i.e. lower

heat flux levels. The correlation for confined boiling of Chowdhury et al [6] tends to over predict the measured values though agreement is still reasonable and consistent over the entire range tested.

Apart from the Kutateladze correlation the conventional pool boiling correlations tend to agree very well with the measurements for the low thermal resistance levels. A possible explanation for this is that these correspond with low levels of heat flux and thus it would be expected that bubble activity would be less rigorous. For higher heat fluxes, where a lower thermal resistance is expected due to increased bubble activity, the correlations of Rohsenow and Kruzhilin under predict the thermal resistance by approximately a factor of two. In the Rohsenhow correlation $C_{s,f}$=0.0147 and n=1 were used as suggested by Vachon et al [26] for water and polished copper. Of all the correlations tested, the Labuntsov correlation performs best for this water-charged thermosyphon over the range of heat fluxes tested. Even still, the Kutateladze correlation shows the best agreement for the low thermal resistance levels i.e. for high heat fluxes.

For the tests with a 0.6ml of water there will exist a region of approximately l_p~½ l_e in which nucleate pool boiling is occurring as well a region of approximate length l_p~½ l_e where evaporation is occurring across a thin liquid film. Based on the above discussion the Labuntsov correlation (Table 3), can be applied for the pool boiling region with adequate accuracy. For the thin film region it is less clear as to how to model the heat transfer. For a first approximation and for a short thin film region it would seem reasonable to apply Nusselt's theory, albeit for evaporation, for a constant film thickness equal to that of the thickness associated with the exit of the condenser section. This would result in a heat transfer coefficient predicted by the expression,

$$h_f = \left(\frac{\rho_l (\rho_l - \rho_v) g k_l^3 h_{fg}}{4 \mu_l (T_v - T_c) l_c} \right)^{\frac{1}{4}}$$

(11)

Referring to Fig. 5 it is evident that using Labuntsov correlation (Table 3) in the pool boiling region, Eq. 11 in the thin film region and considering the two to act thermally in parallel shows good agreement with the measurements. The correlation developed by El-Genk and Saber [3] which accounts for nucleate boiling in the thin film for high heat fluxes is also plotted in the figure showing a notable under prediction of the measurements, suggesting that, for the scenario here, nucleate boiling may not be

occurring within the film. This correlation can be expressed as a ratio with the Kutateladze correlation, h_{Ku}, (Table 3) as,

$$\frac{h_{NB}}{h_{Ku}} = 1.662 \left(\frac{\mu_l}{(\sigma g \sqrt{\sigma / g(\rho_l - \rho_g)})^{0.5}} \right)^{-0.337}$$ (12)

It is unclear as to why this under prediction occurs though it may be due to the working fluid (water was not a working fluid used in the correlation development), heater surface morphology, confinement or other thermal-hydraulic effects that are not immediately obvious without proper visualization capabilities.

5.2.1. Condenser Section

Various aspects of condensation heat transfer have been studied both experimentally and theoretically. Although definitions vary, the condensation heat transfer can be characterized by a relation between Nusselt number, Nu, and the film Reynolds number, Re_f. For this study these are defined respectively as,

$$Re_f = \frac{4Q}{\pi D h_{fg} \mu}$$ (13)

and,

$$Nu = \frac{h_c l_c}{k_l}$$ (14)

Within the laminar regime it is very common to use the area averaged version of Nusselt's theory for filmwise condensation on a horizontal flat plate [7;8]. The average heat transfer coefficient for this model is,

$$h_c = 0.943 \left(\frac{\rho_l (\rho_l - \rho_v) g k_l^3 h_{fg}}{\mu_l (T_v - T_c) l_c} \right)^{\frac{1}{4}}$$ (15)

In other cases simple empirical modifications of this theory are also implemented [9;27]. As outlined by Gross [8], agreement between measurements and Nusselt's theory is not assured with it often over predicting the measurements at low heat fluxes (low Re_f) whilst under predicting at higher heat fluxes (high Re_f). Correlations that account for the improved heat transfer due to waviness of the surface or turbulence can improve the agreement between the correlations and the measurements for a broad range of working fluids in the higher Re_f range. Correlations to account for the notable discrepancy at lower Re_f is not provided in [8], though Hashimoto and

Kaminaga [9], more recently, proved that this degradation in the heat transfer is due to fluid entrainment. Taking into account the fact that at lower heat fluxes the film thickness is smaller, combined with the knowledge that the amount of entrainment increases as the density ratio increases, Hashimoto and Kaminaga [9] proposed the following correlation,

$$h_c = 0.85 \, \mathrm{Re}_f^{0.1} \exp\left(-0.000067 \frac{\rho_l}{\rho_v} - 0.6\right)\left\{0.943\left(\frac{\rho_l(\rho_l - \rho_v)gk_l^3 h_{fg}}{\mu_l(T_v - T_c)l_c}\right)^{\frac{1}{4}}\right\} \qquad \textbf{(16)}$$

Eq. 16 is ostensibly a modification factor multiplied with the Nusselt equation expressed in Eq. 15.

Fig. 6 shows the agreement with the present experimentally determined heat transfer coefficients with that of the above two relations. Consistent with the measurements of Hashimoto and Kaminaga [9], the Nusselt equation notably over predicts the measurements at low Re_f. For high Re_f the agreement with Nusselt's theory is quite good. From the figure it is also evident that the experimental measurements follow very closely the Nu versus Re_f dependency of the Hashimoto and Kaminaga correlation. In particular, there is a notable change in the power law dependency of Nu on Re_f at low and high Reynolds numbers indicating a change in the mechanism(s) of heat transfer. A regression analysis using the same form as Eq. 16 was performed on these measurements producing the following correlation for the condenser heat transfer coefficient;

$$h_c = 0.85 \, \mathrm{Re}_f^{0.1} \exp\left(-0.000067 \frac{\rho_l}{\rho_v} - 0.14\right)\left\{0.943\left(\frac{\rho_l(\rho_l - \rho_v)gk_l^3 h_{fg}}{\mu_l(T_v - T_c)l_c}\right)^{\frac{1}{4}}\right\} \qquad \textbf{(17)}$$

This correlation is also plotted in Fig. 6 showing very good agreement with the measurements. It should be noted that only one term in the argument of the exponential term showed any significant change compared with Eq. 16 indicating the possibility that that this term may be rig/thermosyphon dependent whilst the others are more general in nature although more experiments need to be performed to confirm this.

5.2.1. Overall Thermal Resistance

The net thermal resistance of the thermosyphon is determined by adding the thermal resistances of each the evaporator and condenser sections since they are thermally in series. This gives.

$$R = R_e + R_c \tag{18}$$

The experimental results and predicted results using the Labuntsov correlation, Table 3, and Eq. 17 are plotted in Fig. 7 for the fill volume of 1.8 ml with similar agreement being observed with the 0.6 fill volume (not shown). Evidently the measured and predicted thermal resistance curves agree very well. It is also apparent that the thermal resistance depends strongly on the imposed power varying between R=1.1 ^{o}C/W at Q=21 W to R=0.14 ^{o}C/W at Q=260 W. Also plotted in the figure is the predicted contribution of both the evaporator and condenser thermal resistances. It is clear that the steep increase in the net thermal resistance with decreasing heat flux is a compound influence of both R_e and R_c increasing, which has not been reported in previous investigations. For the evaporator section this is due to less rigorous nucleate boiling whereas in the condenser section this is a very likely due to liquid entrainment which deteriorates the heat transfer.

5.2 FC-77, FC-84 and FC-3284 Charged Thermosyphons

As mentioned earlier, some sensitive applications may require that liquids other than water be used as working fluids in thermosyphons. Further to this, the different thermophysical properties may in some cases be favourable; in particular there is some evidence to suggest that at low temperatures water gives less satisfactory heat transfer performance compared with low boiling point refrigerants [10].

Fig. 8 illustrates the temperature distribution along the FC-84 charged thermosyphon for varying applied power loads. The trends observed for this fluid are, on the most part, very similar to those of the FC-77 and FC-3284 charged units. At the lower power settings (<40 W) the temperature distributions are comparable with the water charged thermosyphon with the same fluid loading signifying similar thermal performance below 40 W. However, beyond approximately 40W the rate at which the evaporator temperature rises with applied power is significantly higher than the water charged unit. To a lesser extent, the opposite is true for the condenser temperatures

signifying that the boiling dynamics of the Flourinert[TM] liquids is affected more than the condensing dynamics. Even still, the net effect is an increase in the temperature differential between the evaporator and condenser sections for a given power level which results in an increase in the net thermal resistance of the Flourinert[TM] charged thermosyphons compared with water. This is illustrated more clearly in Fig. 9 where R_e (Fig. 9a), R_c (Fig. 9b), and R_{exp} (Fig. 9c), are plotted for all for fluids tested.

From Fig. 9c it is immediately apparent that for the lower power settings these thermosyphons show the same qualitative trends with an increase in the total thermal resistance with decreasing power due to the boiling and condensation dynamics as discussed earlier. With regards to the overall thermal performance, the FC-84 charged thermosyphon, the lowest boiling point fluid tested, outperforms all of the other working fluids, including water, for power levels below approximately 30W. Figs 8a and 8c show that this is a consequence of improved heat transfer in both the evaporator and condenser sections. The other two Flourinert[TM] liquids with boiling points near or above the boiling point of water tend to perform worse than water in this region. Overall, the highest boiling point fluid, FC-2383 performs worst.

Compared with water, the thermal performances of the FC-84, FC-77 and FC-3283 thermosyphons were found to degrade significantly for power levels exceeding approximately 30W-40W. This was determined to be a result of the thermosyphons reaching the counter-flow entrainment limit. This limit can be predicted using the expression [28],

$$Q_{\max} = A_{cs} h_{fg} Ku(\rho_v)^{0.5} \left[\sigma g(\rho_l - \rho_v)\right]^{0.25} \tag{19}$$

where Ku is the Kutateladze number [28]. Utilizing Eq. 19 the entrainment limit for the FC-84, and FC-77 were determined to be 38.4 W and 44W, respectively. Referring to Fig.8a and 8c, these predicted entrainment limits are in good agreement with the experiments, which reached a local minimum at approximately 30 W and 40W for FC-84 and FC-77 respectively. Insufficient thermophysical property information is available to perform this calculation for FC-3283. When the entrainment limit is reached and exceeded the liquid flow back to the evaporator is impeded causing deterioration in the heat transfer and the observed elevation in the evaporator wall temperature for the Flourinert[TM] fluids. For the condenser, a more conventional asymptotic decrease in the thermal resistance values is observed for the Flourinert[TM] fluids. It should be noted that the counter-flow entrainment limit for the

water-charged thermosyphon was above 400W which explains why the water-charged thermosyphon did not fail before the maximum 300 W capacity of this experimental apparatus.

6. Conclusions

A small diameter and compact thermosyphon was tested experimentally with four different working fluids: water, FC-84, FC-77 and FC-3283. For the water charged unit, the available pool boiling and combined pool boiling-thin film evaporation expressions showed good predictions for the evaporator section whilst the Nusselt theory for filmwise condensation over-predicted the measured condensation heat transfer data at low powers, though this improved with increasing power levels. In the condenser section, the measured data followed very closely the trend of the Hashimoto and Kaminaga correlation [9] suggesting that liquid entrainment affects the condensation heat transfer for low power levels. A simple modification of this theory shows excellent quantitative agreement with the measurements of this study.

For power levels below approximately 30-40W, the thermosyphon charged with the lowest boiling point liquid, FC-84, was the only Flourinert^{TM} liquid tested that was measured to outperformed the water charged unit for the same fluid loading, possibly due to its lower boiling temperatures. Generally, water outperformed the Flourinert^{TM} liquids, in particular above approximately 40 W where the liquid entrainment limit compromises the performance of the Flourinert^{TM} charged thermosyphons. Even still, the Flourinert^{TM} liquids FC-84 and FC-77 offer adequate thermal performance below 40 W and offer the added benefit of being dielectric, which may be beneficial in some circumstances.

References

[1] S.H.Noie. Heat transfer characteristics of a two-phase closed thermosyphon, Applied Thermal Engineering, 25, (2005) 495-506.

[2] D.A.Reay, and P.A.Kew, Heat Pipes, 5th Edition, Butterworth-Heinemann, Oxford, 2006.

[3] M.S.El-Genk, H.H.Saber. Heat transfer correlations for liquid film in the the evaporator of enclosed, gravity assisted thermosyphons, Journal of Heat Transfer, 120, (1998) 477-484.

[4] W.M.Rohsenow. A method of correlating heat transfer data for surface boiling of liquids, Transactions of the ASME, 74, (1952) 969-976.

[5] S.S.Kutateladze. Heat Transfer and Hydrodynamic Resistance, in: Energoatomizdat Publishing House, Moscow, Russia, 1990.

[6] F.Md.Chowdhury, F.Kaminaga, K.Goto, K.Matsumura. Boiling Heat Transfer in a Small Diameter Tube below Atmospheric Pressure on a Natural Circulation condition, J.of Japan Association for Heat Pipe, 16, (1997) 14-16.

[7] M.Shiraishi, K.Kikuchi, T.Yamanishi. Investigation of Heat Transfer Characteristics of a Two-Phase Closed Thermosyphon, Heat Recovery Systems, 1, (1981) 287-297.

[8] U.Gross. Reflux condensation heat transfer inside a closed thermosyphon, Int.J.Heat Mass Transfer, 35, (1992) 279-294.

[9] H.Hashimoto, F.Kaminaga. Heat transfer characteristics in a condenser of closed two-phase thermosyphon: Effect of entrainment on heat transfer deterioration, Heat Transfer-Asian Research, 31, (2002) 212-225.

[10] H.Li, A.Akbarzadeh, P.Johnson. The thermal characteristics of a closed two-phase thermosyphon at low temperature difference, Heat Recovery Systems and CHP, 11, (1991) 533-540.

[11] B.S.Larkin. An experimental study of the two-phase thermosyphon tube, 70-CSME-6 (EIC-71-MECH 8), 14, (1971).

[12] Y.Lee, U.Mital. A two-phase closed thermosyphon, International Journal of Heat and Mass Transfer, 15, (1972) 1695-1707.

[13] F.E.Andros. Heat Transfer Characteristics of the Two-Phase Closed Thermosyphon (Wickless Heat Pipe) Including Direct Flow Observation. Ph.D.Dissertation . 1980.

[14] I.Sauciuc, A.Akbarzadeh, P.Johnson. Characteristics of two-phase closed thermosyphons for medium temperature heat recovery applications, Heat Recovery Systems and CHP, 15, (1995) 631-640.

[15] T.Wadowski, A.Akbarzadeh, P.Johnson. Hysteresis in thermosyphon-based heat exchangers and introduction of a novel triggering system for low-temperature difference heat-recovery applications, Heat Recovery Systems and CHP, 11, (1991) 523-531.

[16] H.Z.Abou-Ziyan, A.Helali, M.Fatouch, M.M.Abo El-Nasr. Performance of stationary and vibrated thermosyphon working with water and R134a, Applied Thermal Engineering, 21, (2001) 813-830.

[17] K.S.Ong, M.Haider-E-Alahi. Performance of a R-134a-filled thermosyphon, Applied Thermal Engineering, 23, (2003) 2373-2381.

[18] Y.J.Park, H.K.Kang, C.J.Kim. Heat transfer characteristics of a two-phase closed thermosyphon to the fill charge ratio, International Journal of Heat and Mass Transfer, 45, (2002) 4655-4661.

[19] Y.J.Park, C.J.U.Kim, S.E.Hong. A study of the heat transfer characteristics of an FC-72(C 6F14) two-phase closed thermosyphon with helical grooves on the inner surface, Heat Transfer Engineering, 25, (2002) 60-68.

[20] H.Imura, H.Kusada, J.Oyata, T.Miyazaki, N.Sakamoto. Heat transfer in two-phase closed-type thermosyphons, Transactions of Japan Society of Mechanical Engineers, 22, (1977) 485-493.

[21] D.A.Labuntsov. Heat transfer problems with nucleate boiling of liquids, Thermal Engineering, 19, (1972) 21-28.

[22] G.N.Kruzhilin. Free-convection transfer of heat from a horizontal plate and boiling liquid. 58, 1657-1660 (in Russian). 1947.

[23] I.L.Pioro, W.Rohsenow, S.S.Doerffer. Nucleate pool-boiling heat transfer. II: assessment of prediction methods, International Journal of Heat and Mass Transfer, 47, (2004) 5045-5057.

[24] K.Stephan, M.Abdelsalam. Heat transfer correlations for natural convection boiling, Int.J.Heat Mass Transfer, 23, (1980) 73-87.

[25] H.Jouhara, A.J.Robinson. An Experimental Study of Small Diameter Wickless Heat Pipes Operating in the Temperature Range 200ºC to 450ºC, Heat Transfer Engineering, 30, (2009).

[26] R.I.Vachon, G.H.Nix, G.E.Tanger. Evaluation of constants for Rohsenow pool boiling correlation, Journal of Heat Transfer, 90, (1968) 239-247.

[27] T.Kiatsiriroat, A.Nuntaphan, J.Tiansuwan. Thermal performance enhancement of thermosyphon heat pipe with binary working fluids, Experimental Heat Transfer, 13, (2000) 137-152.

[28] ESDU (Engineering Sciences Data Unit), Heat Pipes - performance of two-phase closed thermosyphons. (No. 81038C). (1983).

Figure 1: Two-phase closed thermosyphon

Figure 2: Schematic diagram of thermosyphon test rig

Figure 3: Temperature distribution along water-filled thermosyphon for varying power loads for V=1.8 ml working fluid.

Figure 4: Predicted and experimentally determined thermal resistance values for the evaporator section for full pool boiling mode with V=1.8 ml water (filled markers indicate correlations developed specifically for thermosyphons).

Figure 5: Predicted and experimentally determined thermal resistance values for the evaporator section of the thermosyphon for V=0.6 ml working fluid.

Figure 6: Predicted and experimentally determined thermal resistance values for the condenser section of the thermosyphon.

Figure 7: Predicted and experimentally determined thermal resistance values for the condenser section of the thermosyphon.

Figure 8: Temperature distribution along FC84-filled thermosyphon for varying power loads.

Figure 9: Thermal resistance versus power throughput for water, FC-84, FC-77 and FC-3283 filled thermosyphons.

Table 1: Thermophysical properties of test liquids at 25ºC

Table 2: Experimental uncertainty of thermal resistance for increasing power level

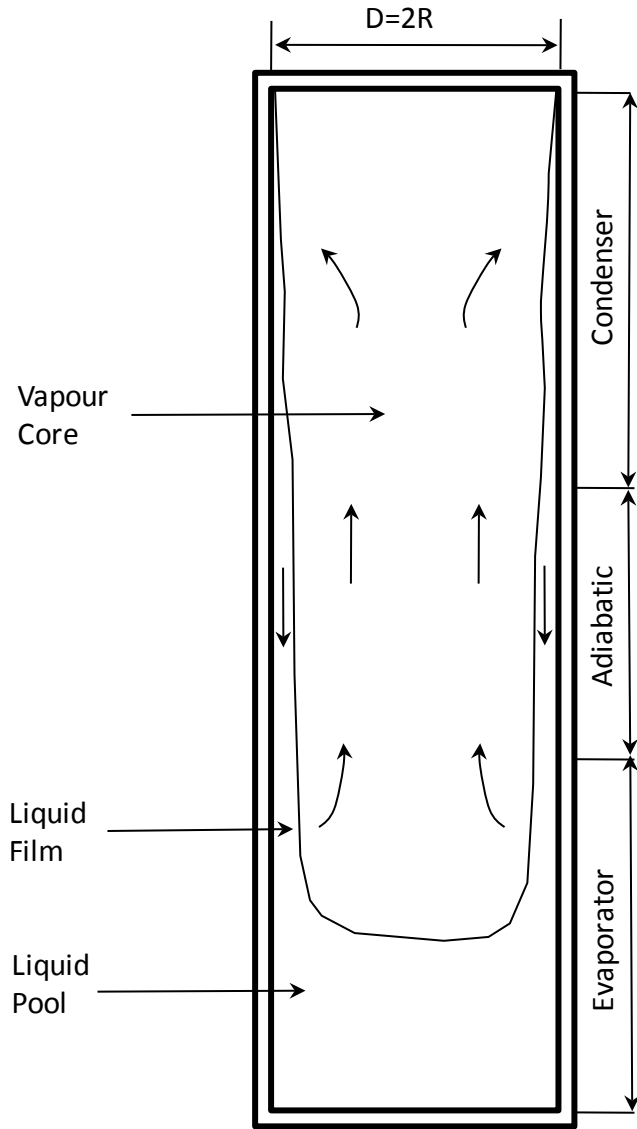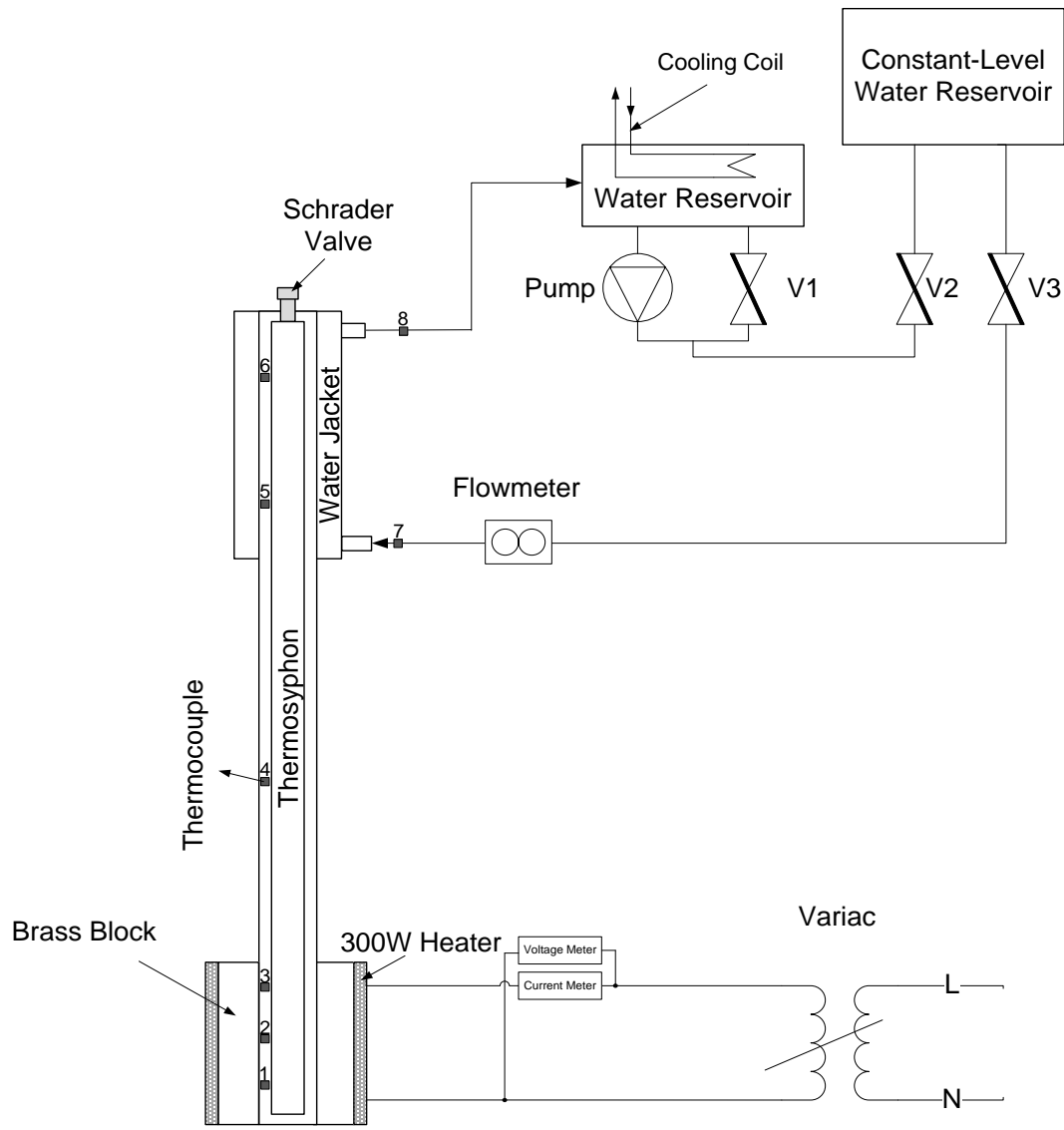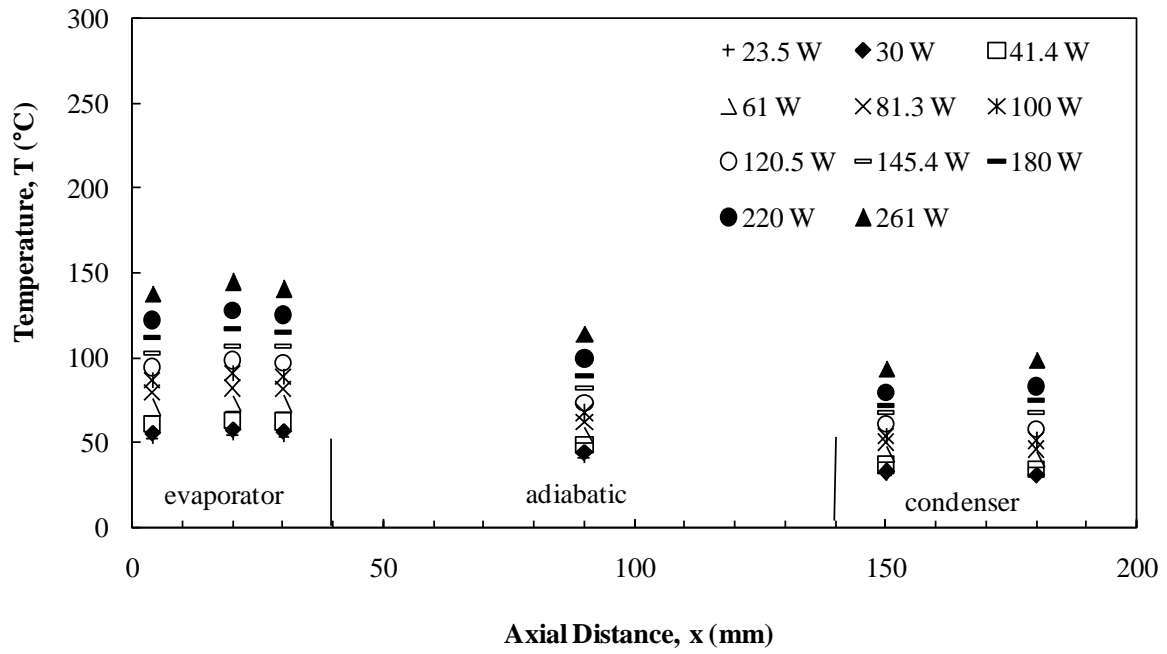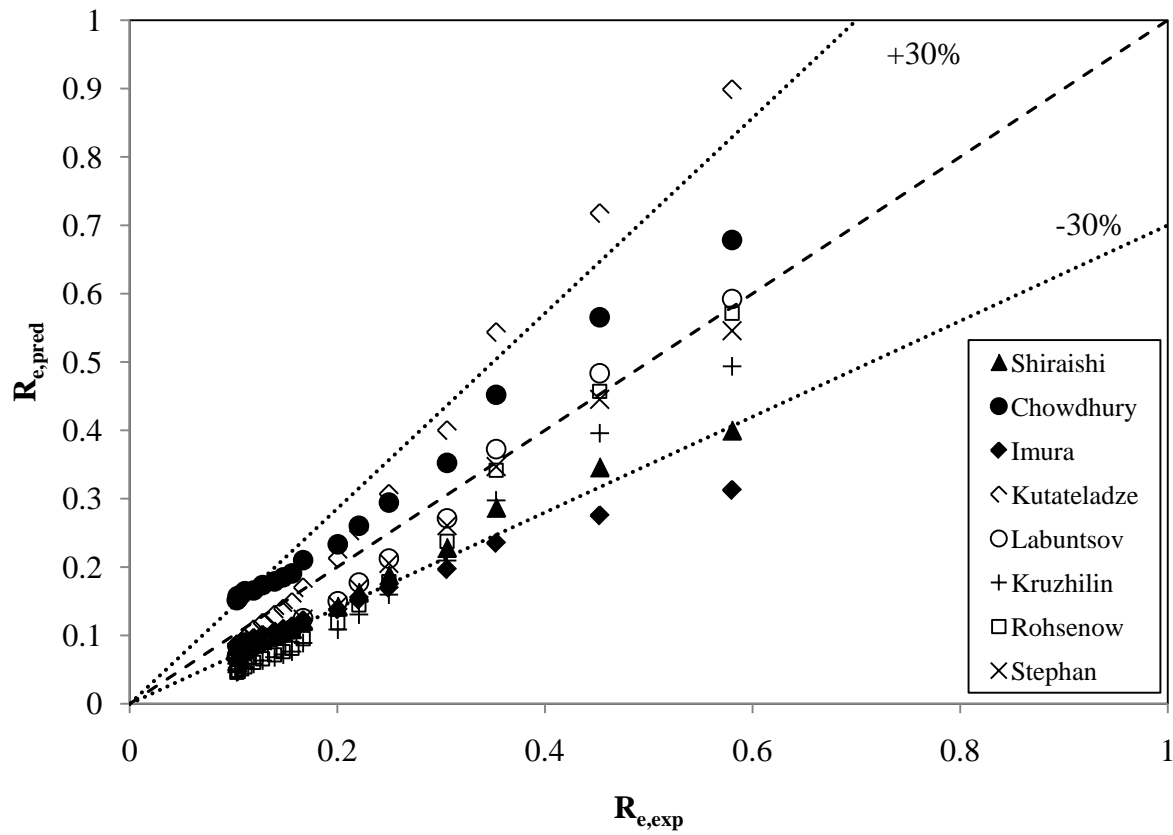Table 3: Nucleate pool boiling heat transfer correlations

Figure 1: Two-phase closed thermosyphon

Figure 1: Schematic diagram of thermosyphon test rig

Figure 1: Temperature distribution along water-filled thermosyphon for varying power loads for V=1.8 ml working fluid.

Figure 1: Predicted and experimentally determined thermal resistance values for the evaporator section for full pool boiling mode with V=1.8 ml water (filled markers indicate correlations developed specifically for thermosyphons).
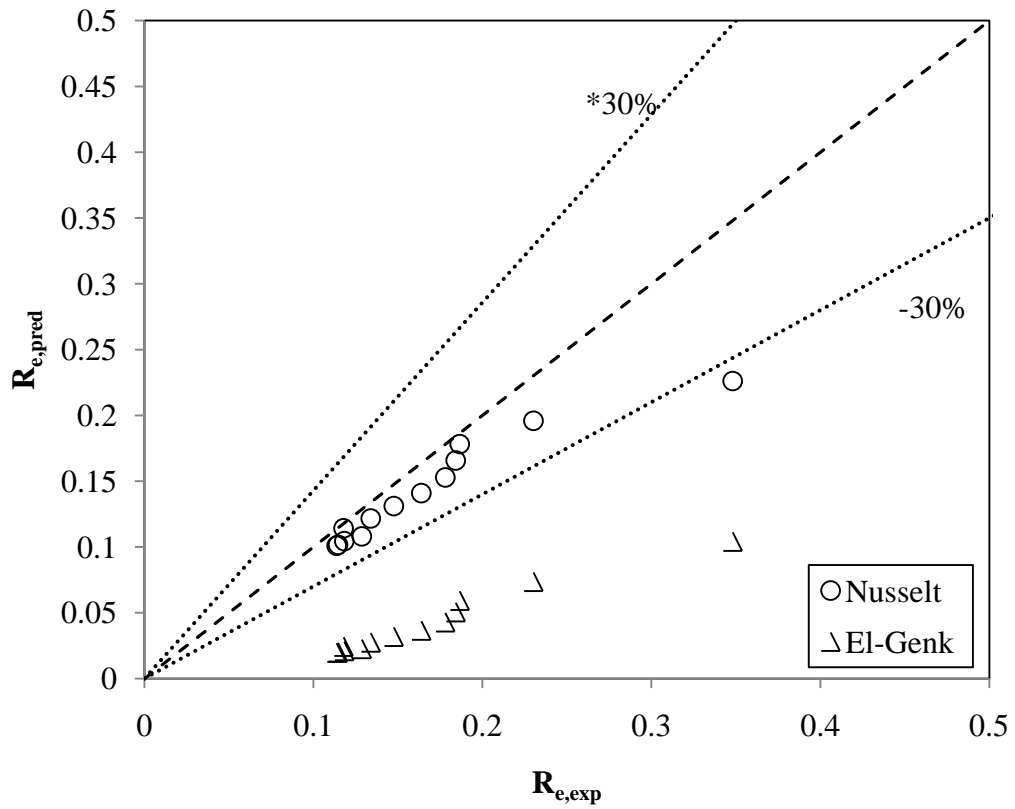
Figure 1: Predicted and experimentally determined thermal resistance values for the evaporator section of the thermosyphon for V=0.6 ml working fluid.
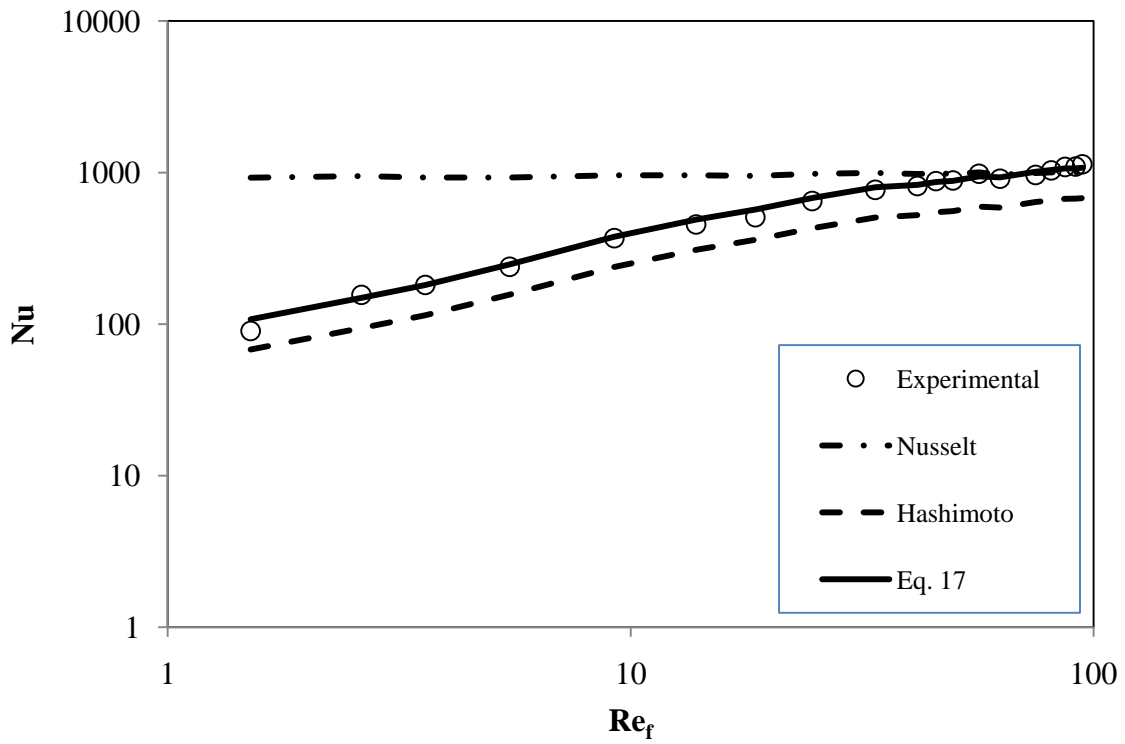
Figure 1: Predicted and experimentally determined dimensionless heat transfer coefficient values for the condenser section of the thermosyphon.
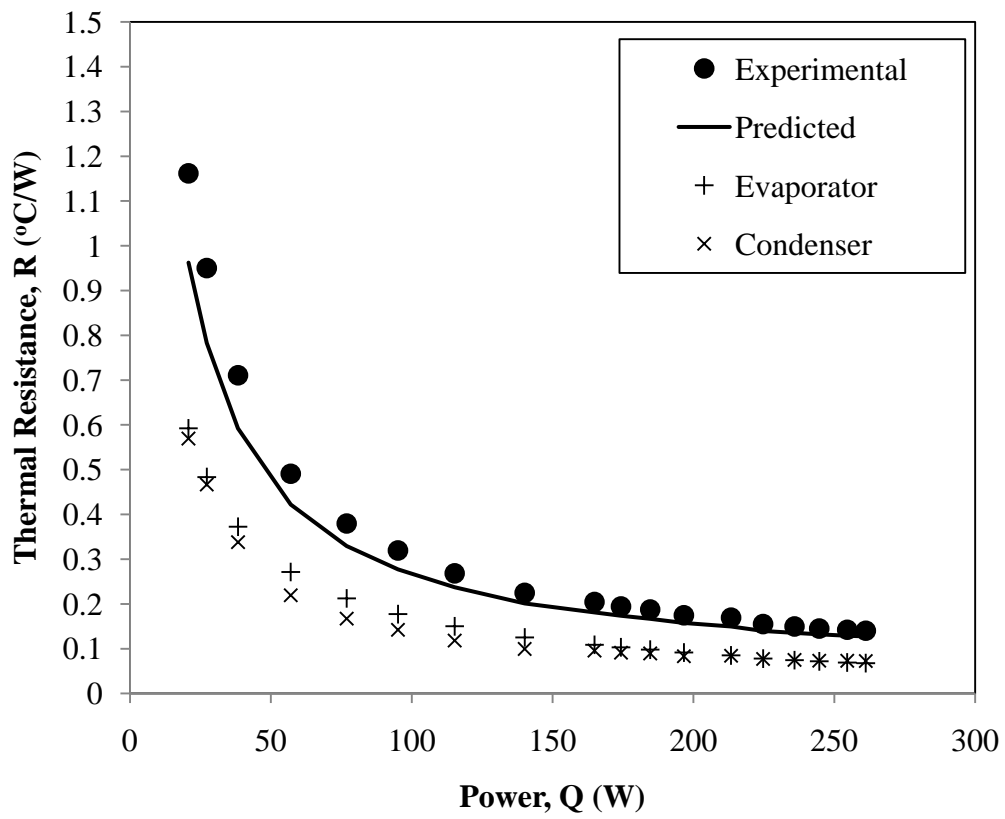
Figure 1: Overall thermal resistance values for the for the 1.8 ml water filled thermosyphon.
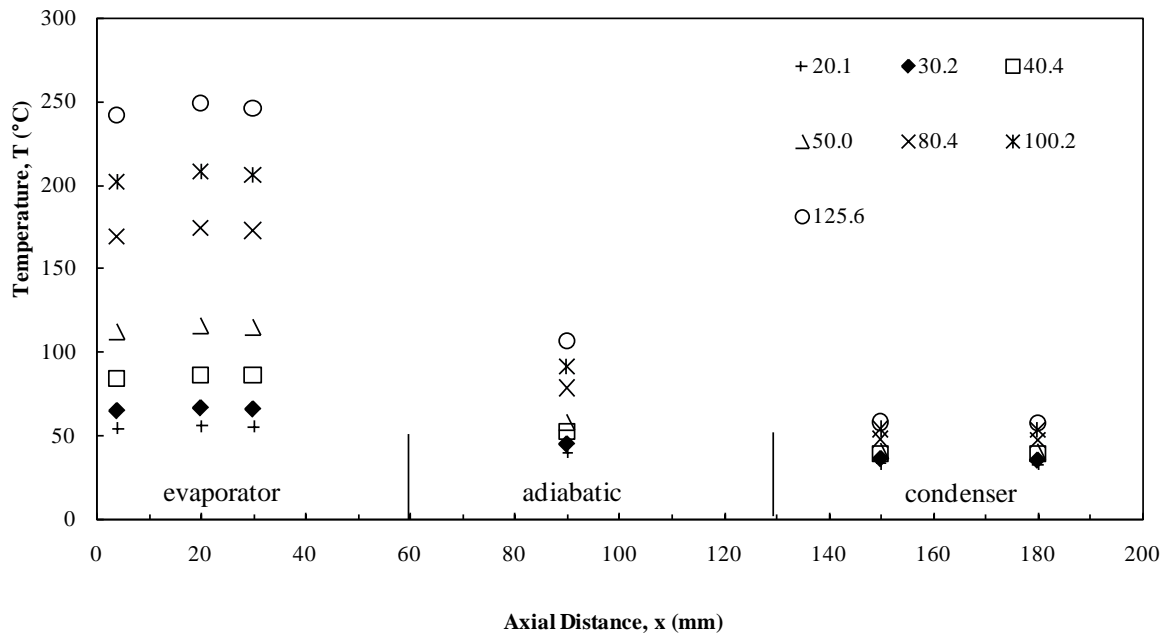
Figure 1: Temperature distribution along FC84-filled thermosyphon for varying power loads.
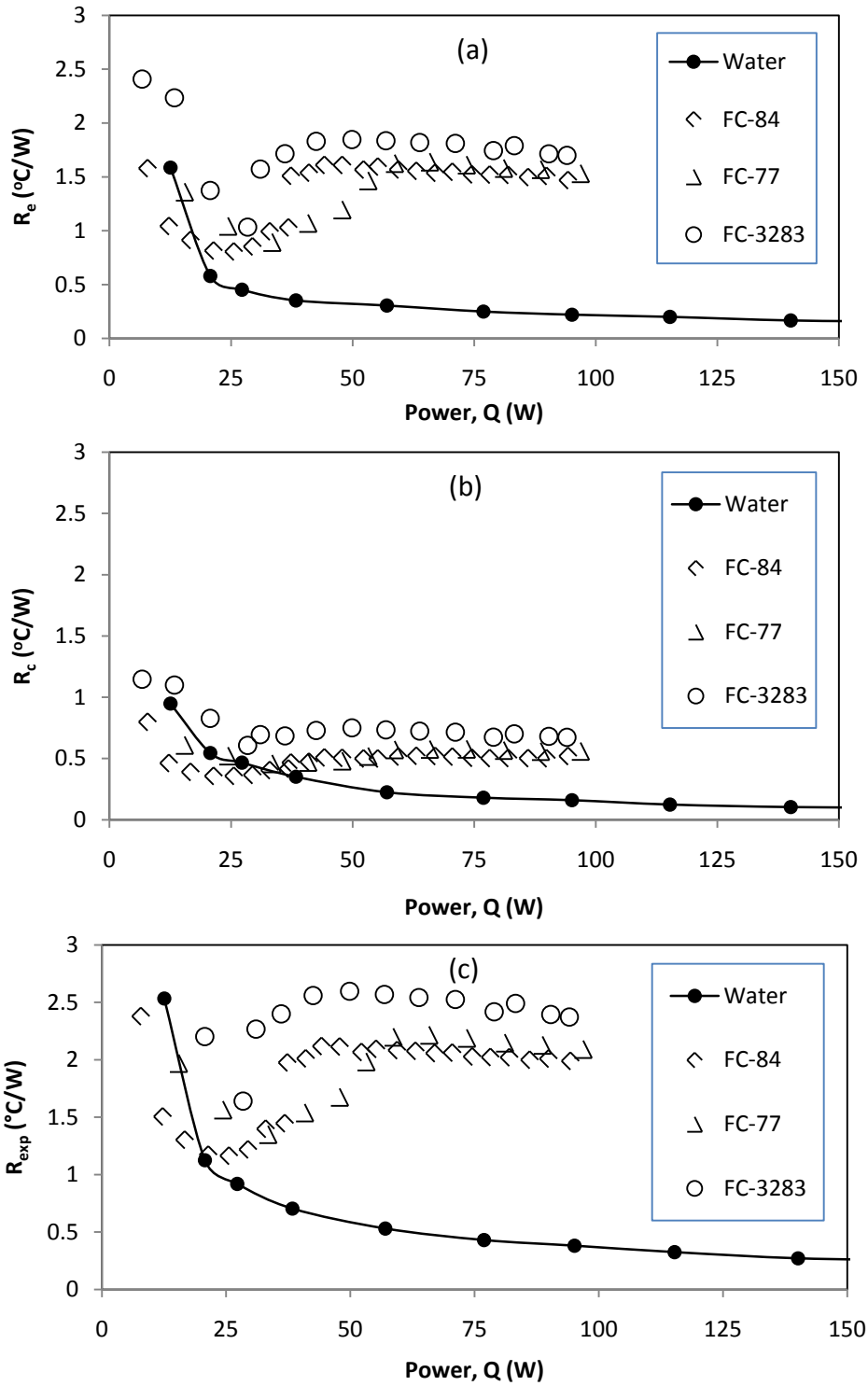
Figure 1: Thermal resistance versus power throughput for water, FC-84, FC-77 and FC-3283 filled thermosyphons.

Table 1: Thermophysical properties of test liquids at 25ºC

Fluid	Molecular Formula	Boiling point (1 atm)	Liquid Density (kg/m^3)	Latent Heat (J/g)	Thermal Conductivity (W/mºC)	Surface Tension (N/m)	Viscosity (Ns/m^2)
Water	H_2O	100 ºC	997	2455	0.607	0.0727	9.6 x 10^{-4}
FC-84	$C_7 F_{16}$	80 ºC	1730	90	0.060	0.012	9.1 x 10^{-4}
FC-77	Blend of 50% $C_8 F_{18}$ and 50% $C_8 F_{16} O$	97 ºC	1780	89	0.063	0.013	13 x 10^{-4}
FC-3283	$(C3F7)_3N$	128 ºC	1820	78	0.066	--	14 x 10^{-4}

Table 2: Experimental uncertainty of thermal resistance for increasing power level

Power, Q	23.5 W	60 W	120W	200W
Uncertainty in R_{exp}	16%	14%	12%	12%

Table 3: Nucleate pool boiling heat transfer correlations

Imura et al [20]	$h_e = 0.32 \left(\dfrac{\rho_l^{0.65} k_l^{0.3} C_{pl}^{0.7} g^{0.2}}{\rho_v^{0.25} h_{fg}^{0.4} \mu_l^{0.1}} \right) \left(\dfrac{P_v}{P_{atm}} \right)^{0.3} q^{0.4}$
Shiraishi et al [7]	$h_e = 0.32 \left(\dfrac{\rho_l^{0.65} k_l^{0.3} C_{pl}^{0.7} g^{0.2}}{\rho_v^{0.25} h_{fg}^{0.4} \mu_l^{0.1}} \right) \left(\dfrac{P_v}{P_{atm}} \right)^{0.23} \left(\dfrac{q^{0.4}}{(\pi D l_e)^{0.4}} \right)$
Chowdhury at al [6]	$h_e = 11.43 (\mathrm{Re}_b)^{0.72} (\mathrm{Pr}_l)^{0.42} \left(\dfrac{\rho_v}{\rho_l} \right)^{0.5} \left(\dfrac{d_d}{D} \right) \left(\dfrac{k_l}{d_d} \right)$
Rohsenow [4]	$h_e = \dfrac{q^{2/3}}{\dfrac{C_{s,f} h_{fg}}{C_{pl}} \left\{ \dfrac{L_b}{h_{fg} \mu_l} \right\}^{0.33} \mathrm{Pr}_l^{1.7}}$
Kutateladze [5]	$h_e = 0.44 \left(\dfrac{k_l}{L_b} \right) \left(\dfrac{1 \times 10^{-4} qP}{g h_{fg} \rho_v \mu_l} \dfrac{\rho_l}{\rho_l - \rho_v} \right)^{0.7} \mathrm{Pr}_l^{0.35}$
Labuntsov [21]	$h_e = 0.075 \left[1 + 10 \left(\dfrac{\rho_v}{\rho_l - \rho_v} \right)^{0.67} \right] \left(\dfrac{k_l^2}{\upsilon_l \sigma (T_{sat} + 273.15)} \right)^{0.33} q^{0.67}$
Kruzhilin [22]	$h_e = 0.082 \left(\dfrac{k_l}{L_b} \right) \left(\dfrac{h_{fg} q}{g(T_{sat} + 273.15) k_l} \dfrac{\rho_l}{\rho_l - \rho_v} \right)^{0.7} \left(\dfrac{(T_{sat} + 273.15) C_{pl} \sigma \rho_l}{h_{fg}^2 \rho_v^2 L_b} \right)^{0.33} \mathrm{Pr}_l^{-0.45}$